The ATP permeability of pannexin 1 channels in a heterologous system and in mammalian taste cells is dispensable

Roman A. Romanov[1], Marina F. Bystrova[1], Olga A. Rogachevskaya[1], Vladimir B. Sadovnikov[2], Valery I. Shestopalov[3] and Stanislav S. Kolesnikov[1,*]

[1]Institute of Cell Biophysics, Russian Academy of Sciences, Institutional Street 3, Pushchino, Moscow Region, 142290, Russia
[2]Pushchino Branch of Shemyakin-Ovchinnikov Institute of Bioorganic Chemistry, Science Avenue 6, Pushchino, Moscow Region, 142290, Russia
[3]Bascom Palmer Eye Institute University of Miami Miller School of Medicine, Miami, FL, USA

*Author for correspondence (staskolesnikov@yahoo.com)

Accepted 31 July 2012
Journal of Cell Science 125, 5514–5523

doi: 10.1242/jcs.111062

Summary

Afferent output in type II taste cells is mediated by ATP liberated through ion channels. It is widely accepted that pannexin 1 (Panx1) channels are responsible for ATP release in diverse cell types, including taste cells. While biophysical evidence implicates slow deactivation of ion channels following ATP release in taste cells, recombinant Panx1 activates and deactivates rapidly. This inconsistency could indicate that the cellular context specifies Panx1 functioning. We cloned Panx1 from murine taste tissue, and heterologously expressed it in three different cell lines: HEK-293, CHO and neuroblastoma SK-N-SH cells. In all three cell lines, Panx1 transfection yielded outwardly rectifying anion channels that exhibited fast gating and negligible permeability to anions exceeding 250 Da. Despite expression of Panx1, the host cells did not liberate ATP upon stimulation, making it unclear whether Panx1 is involved in taste-related ATP secretion. This issue was addressed using mice with genetic ablation of the *Panx1* gene. The ATP-biosensor assay revealed that, in taste cells devoid of Panx1, ATP secretion was robust and apparently unchanged compared with the control. Our data suggest that Panx1 alone forms a channel that has insufficient permeability to ATP. Perhaps, a distinct subunit and/or a regulatory circuit that is absent in taste cells is required to enable a high ATP-permeability mode of a native Panx1-based channel.

Key words: Recombinant pannexin 1, Pannexin 1 knockout, ATP secretion, ATP biosensor, Taste cells

Introduction

Ample evidence implicates a number of first messengers and their receptors in mediating afferent output and paracrine/autocrine regulations in the mammalian taste bud. Multiple neuroactive compounds have been identified in this specialized chemosensory organ, including adenosine, aminobutyric acid, ATP, glutamate, norepinephrine, serotonin, and certain peptides (Chaudhari and Roper, 2010). As evidenced by the loss of essentially all gustatory neural responses in P2X2/P2X3 double knockout (KO) mice (Finger et al., 2005), ATP plays a principal role in the transmission of gustatory information from taste cells to afferent nerve fibers. Consistently, taste cells of the type II have been demonstrated to release ATP into intercellular space upon gustatory and electrical stimulation (Huang et al., 2007; Romanov et al., 2007). This entails activation of P2X2/P2X3 receptors on afferent taste nerves (Bo et al., 1999; Kataoka et al., 2006) and a variety of P2X and P2Y receptors on taste cells (Baryshnikov et al., 2003; Kataoka et al., 2004; Bystrova et al., 2006; Huang et al., 2009; Huang et al., 2011). Taste cells of the type II lack conventional synapses (Royer and Kinnamon, 1991; Tabata et al., 1995), but instead release ATP via voltage-gated channels (Huang et al., 2007; Huang et al., 2011; Romanov et al., 2007; Romanov et al., 2008).

It is widely accepted that in addition to connexons, pannexin 1 (Panx1) channels represent a principal conduit for ATP release in cells of multiple types (see for discussion, Dahl and Locovei, 2006; Chaudhari and Roper, 2010; MacVicar and Thompson, 2010; D'hondt et al., 2011). This point of view is based on a strong correlation between ATP release from stimulated cells and Panx1 activity documented in studies of diverse cellular systems. The underlying evidence was obtained with a variety of approaches, including Panx1 blockers, such as carbenoxolone, probenecid, mefloquine, and the mimetic peptide 10Panx1 (Locovei et al., 2006; Huang et al., 2007; Ransford et al., 2009; Sridharan et al., 2010; Woehrle et al., 2010) as well as RNA interference (Ransford et al., 2009; Chekeni et al., 2010; Iwabuchi and Kawahara, 2011) and the genetic ablation of Panx1 (Santiago et al., 2011; Seminario-Vidal et al., 2011; Qu et al., 2011). In the taste bud, Panx1 is expressed in taste cells of all types, including primary chemosensory cells of the type II (Huang et al., 2007; Romanov et al., 2007). Taking into account this finding and strong inhibitory effects of carbenoxolone on ATP release initiated by gustatory stimuli in the taste bud (Huang et al., 2007, Huang et al., 2011; Murata et al., 2010), it is believed that Panx1 channels are mainly responsible for ATP secretion. However, this inference has not been confirmed yet with a physiological analysis of Panx1-null mice.

Biophysical properties of Panx1 channels were elucidated basically from studies of recombinant Panx1 overexpressed in a heterologous system, while Panx1 features in native cells remain

largely unexplored. The multiplicity of functional ion channels and the lack of subtype-specific blockers of Panx1 channels and connexin hemichannels make it difficult to identify these secretory units and to distinguish between them in native cells. To our knowledge, only Gründken et al. reported on the reliable identification of Panx1-mediated currents in mouse hippocampal CA1 neurons. These Panx1 currents activated and deactivated rapidly (Gründken et al., 2011), as is the case with recombinant mouse Panx1 channels (Ma et al., 2009). Meanwhile, the biophysical analysis of ATP release, including the assay of its dependence on membrane voltage, implicates slowly deactivating ATP-permeable channels in mediating ATP secretion in taste cells of the type II (Romanov et al., 2008). Such a kinetic feature was never reported for recombinant Panx1 channels. The above-mentioned inconsistence could be resolved, should gating and other properties of Panx1 depend on cell-specific microenvironment, accessory proteins and/or regulatory systems.

To clarify whether cellular context specifies Panx1 functioning, we cloned Panx1 from the murine taste tissue and expressed it in cells of three different lines, including HEK-293, CHO and neuroblastoma SK-N-SH. We particularly found that Panx1-positive cells of either type exhibited undetectable ATP release upon stimulation. Moreover, taste cells devoid of Panx1 showed apparently unchanged ATP secretion compared to control. Thus, our results indicate that Panx1 expression is not in complete correlation with ATP secretion.

Results

Mouse Panx1 cloned from circumvallate papilla was heterologously expressed in several mammalian cell lines, including neuroblastoma SK-N-SH, CHO and HEK-293. With 140 mM CsCl in the recording pipette and 140 mM NaCl in the bath, non-transfected SK-N-SH, CHO and HEK-293 cells showed at +80 mV the small and weakly potential-dependent whole-cell (WC) currents of 257±62 pA (n=6), 56±10 pA (n=19) and 64±12 pA (n=10) on average, respectively. Cells transfected with the vector only DNA were basically indistinguishable from non-transfected cells by their electrophysiology (data not shown). When cells were loaded with pIRES2-EGFP/Panx1 plasmid, large WC currents with marked outward rectification were recorded 24–48 hours after cell transfection (Fig. 1A–C, upper panels). At 80 mV, SK-N-SH, CHO, and HEK-293 cells showed the steady-state currents of 668±121 pA (n=18), 345±67 pA (n=24) and 569±47 pA (n=68), respectively. The currents were reversibly blocked by CBX (10–50 μM) (Fig. 1A–C, bottom panels) as well as by probenecid (0.5–2 mM) and 5-nitro-2-(3-phenylpropylamino) benzoic acid (NPPB) (200 μM) (supplementary material Fig. S1A,B). The CBX-sensitive component of WC currents, which we attributed to Panx1 activity, was well-detectable at negative voltages (Fig. 1D–F), signifying that Panx1 channels were active at resting potentials. Apparently, SK-N-SH cells were the most effective expression system, in terms of Panx1 current magnitude, compared to CHO and HEK-293 cells (Fig. 1A–C, upper panels). However, unlike

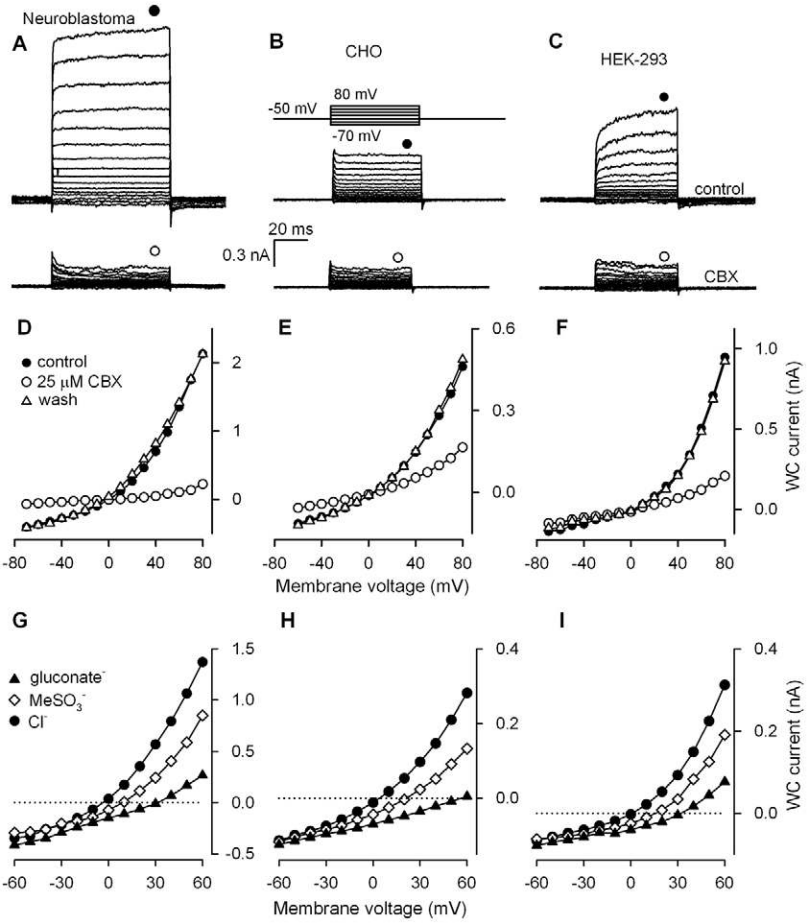

Fig. 1. Representative carbenoxolone-sensitive WC currents recorded from cells of different lines transfected with the pIRES2-EGFP-Panx1 plasmid, including neuroblastoma SK-N-SH (A), CHO (B), and HEK-293 (C) cells. (**A–C**) Cells were held at −50 mV and polarized by 100-ms (SK-N-SH) or 50-ms (CHO and HEK-293) voltage pulses between −70 and 80 mV [upper panel in C]. Bottom panels: whole-cell (WC) currents were recorded in the presence of 25 μM carbenoxolone (CBX). In all cases, cells were perfused with the solution (mM): 140 NaCl, 2 KCl, 1 $CaCl_2$, 1 $MgCl_2$, 10 HEPES-NaOH; the patch pipette contains (mM): 100 CsCl, 0.5 $MgCl_2$, 10 BAPTA-40 CsOH, 10 mM HEPES-CsOH. (**D–F**) I–V curves of steady-state currents shown in A–C, respectively. The current values for generating I–V curves were measured at the moments indicated by the symbols above the current traces. (**G–I**) I–V curves of Panx1 currents with different anions in the bath, as indicated in G. In all cases, 140 mM NaCl+2 mM KCl in the bath was substituted for 140 mM Na-gluconate+2 mM K-gluconate or 140 mM $NaMeSO_3$+2 mM $KMeSO_3$.

control CHO and HEK-293 cells that were basically insensitive to CBX, WC currents in non-transfected SK-N-SH were inhibited by 20–30% in the presence of 10–50 μM CBX. The expression of endogenous Panx1 might account for the CBX-sensitivity of this cell line. On the other hand, HEK-293 cells provided Panx1 expression at a high enough level and also allowed for stable recordings of Panx1-specific currents for 30–40 min and their clear discrimination by sensitivity to CBX. We therefore continued studies of recombinant Panx1 activity in HEK-293 cells in the majority of the subsequent experiments described below.

Typically, Panx1 channels activated quickly, irrespective of an expression system (Fig. 1A–C, upper panels). Certain SK-N-SH and HEK-293 cells (~30% and ~40%, respectively) exhibited Panx1 currents with biphasic kinetics of activation: the current reached a value close (~90%) to the saturating level within few milliseconds but required extra 20–40 ms to achieve the steady-state level (Fig. 1A,C, upper panels). In any event, Panx1 currents deactivated swiftly (Fig. 1A–C, upper panels). It therefore appears that the deactivation kinetics of Panx1 channels is intrinsically rapid.

Anion permeability of Panx1 channels

In each expression system, Panx1 currents reversed at nearly zero voltage with CsCl and NaCl as the main intracellular and extracellular salines, respectively (Fig. 1D,E). Thus, either Panx1 channels are cationic, equally permeable to Cs^+ and Na^+, or those are anionic by nature. When NaCl in the bath was substituted for N-methyl-D-glucamine chloride, reversal potentials of Panx1 currents varied insignificantly (n=5) (supplementary material Fig. S1E). Similar results were reported by Pelegrin and Surprenant (Pelegrin and Surprenant, 2006). In contrast, the substitution of extracellular chloride for a larger anion evidently shifted reversal potentials of Panx1 currents (Fig. 1G–I). These observations leave little doubts that Panx1 channels are rather anionic.

We endeavored to evaluate the permeability of Panx1 channels expressed in HEK-293 cells to a variety of anions. The replacement of bath chloride with methylosulfonate (95 Da) shifted the reversal potential of Panx1 currents to the right by 17.3±2.2 mV on average (n=9). Much larger shifts of 36.5±4.9 mV (n=4), 38.2±3.9 mV (n=6), 40.9±3.1 mV (n=20), and 68.7±1.8 mV (n=7) were elicited by aspartate (131 Da), glutamate (145 Da), gluconate (195 Da) and HEPES (237 Da), respectively (Fig. 1G–I; Fig. 2A–E). Altogether, these observations indicated that Panx1 formed essentially anion channels, at least in the heterologous system. Based on the above estimates and using the Goldman–Hodgkin–Katz formalism for entirely anionic Panx1 channels, the following relative permeability ratios were obtained for the monovalent anions: Cl^-:$MeSO_4$:gluconate:HEPES=1:0.49:0.17:<0.01.

The Cl^- substitution experiments indicated that HEPES might represent the upper size for Panx1 permeants. We examined this possibility in a special series of experiments, wherein extracellular chloride was partially substituted for HEPES, so that $[Cl]_{out}$+$[HEPES]_{out}$=146 mM. To keep intracellular chloride concentration negligibly variable during cell polarization, I–V curves for Panx1 currents were generated by the voltage ramp between −80 mV and 80 mV at the rate of 1 mV/ms. The partial substitution of extracellular chloride with HEPES led to a gradual shift of the Panx1 current reversal potential, depending on concentrations of the bath anions (Fig. 2D). The reversal potential shift versus $-\log[Cl]_{out}$ was nearly linear with the slope of about 58.6 mV (Fig. 2E), the value being remarkably close to the 59.16 mV slope characteristic of the ideal Cl^- selective electrode at 25°C. Thus, although dye loading experiments suggest that Panx1 channels can be permeable for species of up to 1 kDa (MacVicar and Thompson, 2010), their permeability to ions in all tested cell lines seems to be limited by less sizable anions.

Single-channel Panx1 current

When inside-out patches were excised from control non-transfected HEK-293 cells (n=31), none exhibited CBX-sensitive single-channel activity at variable voltages (not shown). In Panx1-positive cells, 26 out of 63 stable inside-out patches

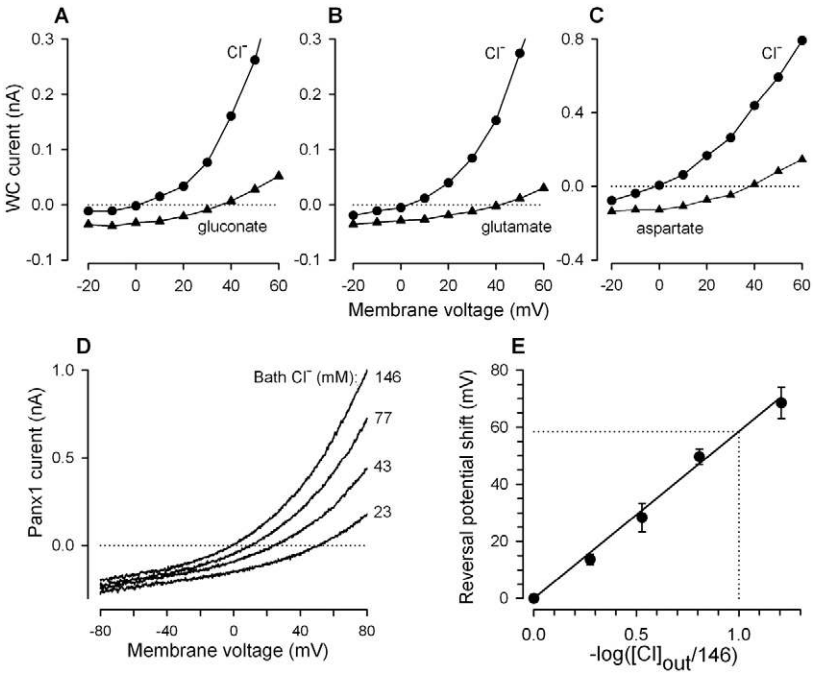

Fig. 2. Panx1-currents in HEK-293 cells recorded with different anions in the bath. (**A**–**C**) Representative I–V curves illustrating shifts of Panx1 current reversal potentials upon replacement of extracellular Cl^- with large anions. Here, 140 mM NaCl+2 mM KCl in the bath was substituted for 140 mM Na-gluconate+2 mM K-gluconate, 140 mM Na-glutamate+2 mM K-glutamate, or 140 mM Na-aspartate+2 mM K-aspartate. The Panx1 current was calculated as the difference between whole-cell (WC) currents with and without 25 μM CBX. (**D**) Panx1 current I–V curves generated by the voltage ramp from −80 mV to 80 mV at different Cl^- concentrations in the bath ($[Cl^-]_{out}$), obtained by the replacement of chloride with HEPES so that $[Cl^-]_{out}$+$[HEPES]_{out}$=146 mM. (**E**) Shift of Panx1 current reversal potential as a function of bath Cl^- concentration. The data are presented as a mean ± S.E. (n=3–7). The solid line corresponds to the equation $\Delta V_r = -58.6 \log([Cl]_{out}/146)$. In A–D, cells were dialyzed as in Fig. 1.

exhibited single channel-like openings blockable with 20 μM CBX (Fig. 3A,C). It is noteworthy that in patches excited from cells with relatively high EGFP fluorescence that was associated with Panx1 expression, channel openings sensitive to CBX were observed more frequently. This convinced us that the CBX-sensitive step-like current events (Fig. 3A) mirrored the abundance of Panx1-channels. In the presence of 20 μM CBX, the open probability P_o of Panx1-channels was markedly reduced compared to control (Fig. 3A,B), while single-channel current magnitude was virtually unchanged (Fig. 3C,D). Particularly at 70 mV, averaged values of $P_o=0.67\pm0.08$ and $P_o=0.12\pm0.03$ ($n=5$) were obtained in control and with 20 μM CBX in the bath, respectively. CBX inhibited Panx1 activity largely by increasing intervals between opening bursts (Fig. 3C).

Interestingly, as a function of membrane voltage, the single Panx1 channel current i was not linear but outwardly rectifying (Fig. 4A). At high negative and high positive voltages, single Panx1 channel current versus membrane voltage was nearly linear with the slopes of 15 pS and 74 pS, respectively (Fig. 4A). When normalized and superimposed, the averaged WC and single-channel Panx1 currents were markedly different at negative voltages (Fig. 4B), indicating that P_o is potential-dependent. Given that the integral current mediated by N identical channels $I=NP_oi$, the factor NP_o at given voltage can be evaluated by the ratio of experimental values of WC and single-channel currents, i.e. $NP_o=I/i$. Based on this relation and using the data presented in Fig. 4B, we calculated normalized NP_o as a function of membrane voltage (Fig. 4C, circles). The experimental values were satisfactorily fitted with the expression (Fig. 4C, solid line):

$$NP_o=\frac{A}{1+B\exp(-V/V_0)}, \quad (1)$$

with $A=30$, $B=62.8$ and $V_0=110$ mV. As follows from this expression, only twofold variation is allowed for the factor NP_o within $-80\div0$ mV, that is, in the physiologically relevant range of membrane voltages. The elucidated voltage dependence of NP_o suggests that the activity of Panx1 channels should be high enough at resting potentials.

Permeability of Panx1 channels to ATP

The ion substitution experiments indicated that Panx1 channels might be impermeable to HEPES (Fig. 2). If so, the ATP anion that is nearly 3 times larger than the HEPES anion should not pass the Panx1 channel as well. On the other hand, the accuracy of measurements of reversal potentials is not high enough to reliably analyze channel permeability to poor permeants. Moreover, ATP blocks Panx1 currents at low millimolar concentrations (supplementary material Fig. S2) (Ma et al., 2009; Qiu and Dahl, 2009). We therefore checked the electrophysiological evidence for negligible ATP permeability of Panx1 channels by assaying ATP release from Panx1-positive HEK-293 cells. In such experiments, released ATP was monitored with COS-1 cells that responded to ambient bath ATP (50 nM–10 μM) with Ca^{2+} transients (Romanov et al., 2007).

To initiate ATP liberation, Panx1-positive HEK-293 cells were dialyzed and depolarized via the patch-clamp electrode containing

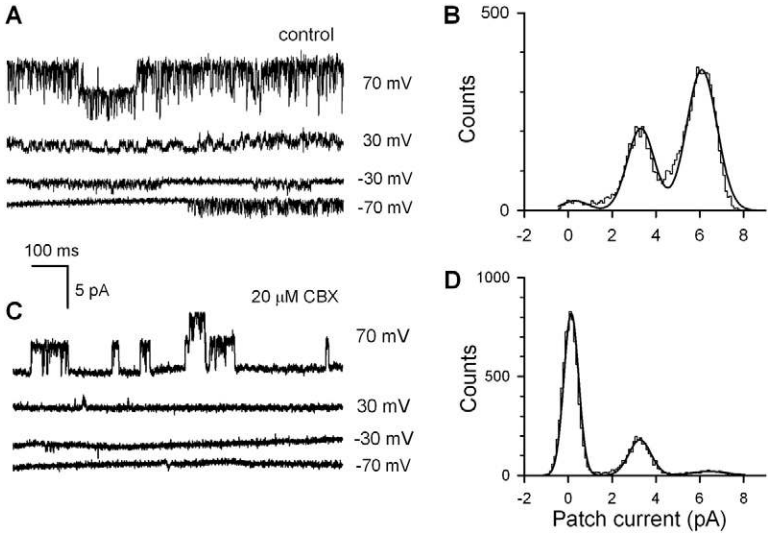

Fig. 3. Single Panx1 channel activity. (**A**,**C**) Single-channel current fluctuations observed at different voltages in control (A), and with 20 μM carbenoxolone (CBX) in the bath (C). An inside-out patch was excised from the plasma membrane of a Panx-positive HEK-293 cell. The patch pipette was filled with the solution (mM): 140 NaCl, 2 KCl, 1 $CaCl_2$, 1 $MgCl_2$, 10 HEPES-NaOH; the bath contains (mM): 140 CsCl, 0.5 $MgCl_2$, 1 EGTA, 10 HEPES-CsOH. (**B**,**D**) Amplitude histograms of patch current recorded at 70 mV in the absence (A) and in the presence of 20 μM CBX in the bath (C) illustrate that two individual channels were active in the patch. The histograms were fitted with the expression (smooth thick lines):

$$N(i)=N_1\exp\left(-\frac{(i-i_1)^2}{2\sigma_1^2}\right)+N_2\exp\left(-\frac{(i-i_1)^2}{2\sigma_2^2}\right)+N_3\exp\left(-\frac{(i-i_3)^2}{2\sigma_3^2}\right)$$

with $N_1=24.5$, $i_1=0.29$ pA, $\sigma_1=0.61$ pA; $N_2=207$, $i_2=3.31$ pA, $\sigma_2=0.62$ pA; $N_3=355$, $i_3=6.09$ pA, $\sigma_3=0.69$ pA in B and $N_1=818$, $i_1=0.14$ pA, $\sigma_1=0.34$ pA; $N_2=180$, $i_2=3.27$ pA, $\sigma_2=0.51$; $N_3=20.4$, $i_3=6.42$ pA, $\sigma_3=0.79$ pA in C. Given that i_3- $i_2=2.78$ pA and i_2 -$i_1=3.02$ pA in B and i_3- $i_2=3.25$ pA and i_2 -$i_1=3.13$ pA in D. It appears that 20 μM CBX did not affect magnitude of the single Panx1 channel current in D.

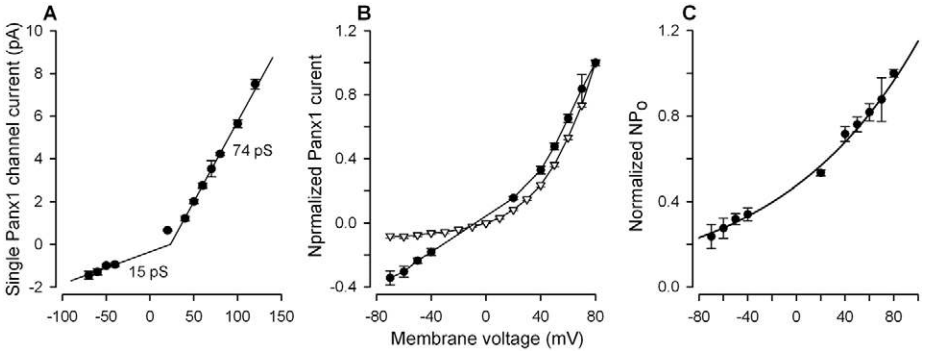

Fig. 4. Voltage dependence of the Panx1 current. (**A**) Single Panx1 channel current versus membrane voltage. The data are presented as a mean ± S.E. (n=6–11). The solid curve represents a combination of two liner dependencies with the slopes of 15 pS and 74 pS at negative and positive voltages, respectively. (**B**) Dependencies of single Panx1 channel current (●) and integral Panx1 current (▽) on membrane voltage. The data are presented as a mean ± S.E. and are normalized on the value of the particular current at 80 mV. (**C**) Voltage dependence of the factor $NP_o=I/I$, calculated using the data in (**B**). The solid curve corresponds to Eqn 1.

2 mM ATP. Fig. 5A illustrates the representative concurrent recordings of WC current from a HEK-293 cell (middle panel) and intracellular Ca^{2+} in a Fluo-4 loaded COS-1 cell (bottom panel). In response to a step-like depolarization from the holding potential of −50 mV to 50–80 mV (Fig. 5A, upper panel), the HEK-293 cell generated CBX-blockable outward currents, indicating marked activity of Panx1 channels (Fig. 5A, middle panel). However, stimulation of Panx1 currents was never accompanied by any evident responses of the ATP-biosensor, which workability was confirmed by the bath application of 100 nM ATP (Fig. 5, bottom panel). Among 34 Panx1-positive HEK-293 cells assayed, none released enough ATP on variable depolarizing voltage to be detectable with the ATP-biosensor. Similar results were obtained with Panx1-positive SK-N-SH (n=9) and CHO (n=7) cells (supplementary material Fig. S3). Meanwhile, ATP liberation from taste cells of the type II was invariably triggered by depolarization via the recording electrode (Fig. 6H) or due to application of 100 mM KCl (data not shown). These observations demonstrate clearly that in HEK-293, CHO, and SK-N-SH cells, Panx1 forms ion channels with insufficient ATP permeability to serve as an effective conduit for ATP release.

ATP release in taste cells from Panx1-null mice

Thus, we found that overexpression of Panx1 in HEK-293, CHO, and SK-N-SH cells did not endow them with the evident ability to liberate ATP on depolarization, the stimulation being usually sufficient to trigger robust ATP release from taste cells (Fig. 5). However, these cell lines might be deficient in certain accessory proteins or channel subunits, which might be present in taste cells and interact with Panx1 to alter its functional properties. Such interactions as well as specific regulatory circuits might dramatically enhance ATP permeability of Panx1-based channels in taste cells. To determine whether Panx1 is the necessary component of ATP secretory machinery in taste cells of the type II, we used mice with genetically ablated Panx1 expression (Dvoriantchikova et al., 2012).

Taste buds and individual taste cells were isolated from CV papillae using both wild-type (WT) and Panx1-null mice. We first assayed ATP secretion with ATP-biosensor at the level of taste buds. Since type II cells are capable of secreting ATP on both taste stimuli and sufficient depolarization (Huang et al., 2007; Romanov et al., 2007; Romanov et al., 2008; Huang and Roper, 2010) taste buds were stimulated by both KCl and tastants. In a typical experiment, we selected a poorly dissociated taste bud and placed it nearby a COS-1 cell responsive to ATP using a patch pipette (Fig. 6A,C, left panels).

In all experiments with taste buds from CV papillae of WT mice (n=26) (Fig. 6A, left panel), a brief application of 70–100 mM KCl to an assayed bud liberated ATP, judging by an ATP-sensor response (Fig. 6B, left panel). It is noteworthy that

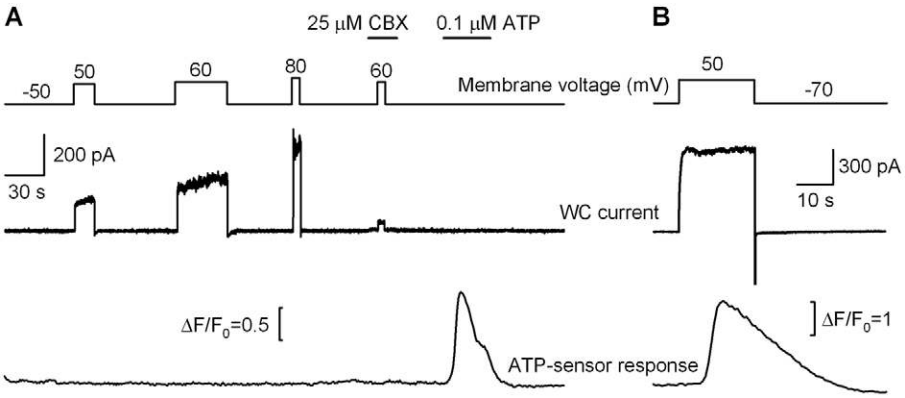

Fig. 5. Assay of ATP release in Panx1-positive HEK-293 cells. (**A**) Representative concurrent recordings of a whole-cell (WC) current from a HEK-293 cell (middle panel) and fluorescence from a nearby Fura-4-loaded COS-1 cell (bottom panel). The upper panel illustrates the time course of holding potential and moments of bath application of 25 μM CBX and 100 nM ATP. (**B**) Depolarization (upper panel) of a type II cell from a wild-type (WT) CV papilla elicited a large outward current (middle panel), followed by stimulation of the ATP-biosensor due to ATP liberation (bottom panel). The perforated patch approach was employed. In (**A**) and (**B**), cells were perfused with the solution (mM): 140 NaCl, 2 KCl, 1 $CaCl_2$, 1 $MgCl_2$, 10 HEPES-NaOH. In (**A**), the patch pipette contains (mM): 100 CsCl, 2 MgATP, 10 BAPTA-40 CsOH, 10 mM HEPES-CsOH. In (**B**), the patch pipette contains (mM): 140 CsCl, 0.5 $MgCl_2$, 1 EGTA, 0.1 EDTA, 10 HEPES-CsOH, 400 μg/ml Amphotericin B.

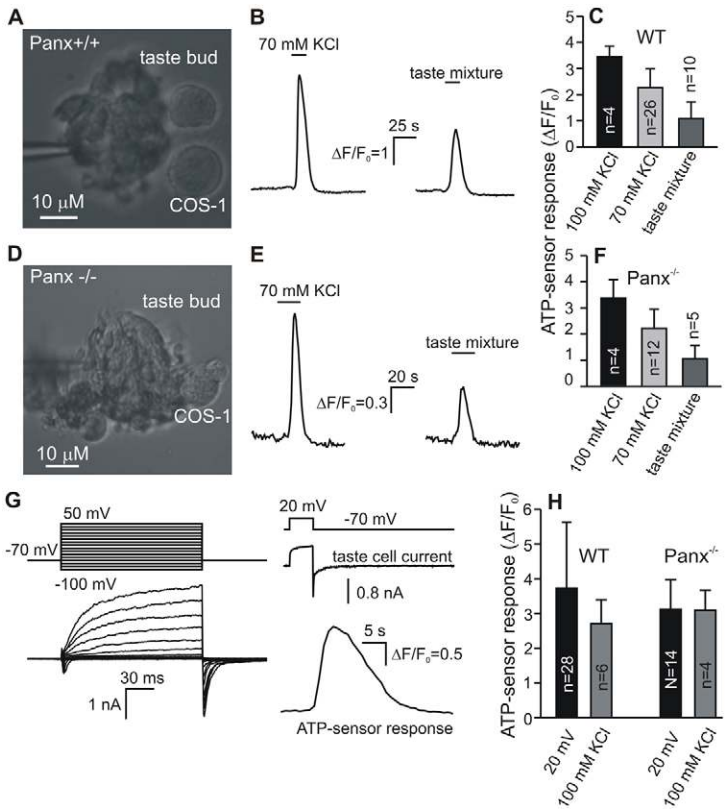

Fig. 6. Assay of ATP release in Panx1 knockout taste cells. (**A**,**D**) Taste buds from a WT CV papilla (A) and from Panx$^{-/-}$ CV papilla (D) that were fixed by the patch pipette, with nearby Fluo-4 loaded COS-1 cells serving as ATP-sensors. (**B**,**E**) ATP-sensor responses on stimulation of the taste bud (A,D) by 70 mM KCl, or by the taste mixture of 100 μm cycloheximide, 100 μm neotam, and 300 μm SC45647. (**C**,**F**) Summary of experiments with wild-type (WT) taste buds (n=27) and Panx$^{-/-}$ taste buds (n=14) assayed as in A,D, and stimulated by KCl (70 and/or 100 mM) and by the taste mixture. The data are presented as a mean ± s.d. For both WT and Panx$^{-/-}$ taste buds, ATP, which was liberated on stimulation with 100 mM KCl, 70 mM KCl, or the taste mixture, elicited statistically different (P<0.05, Student's t-test) responses of the ATP-biosensor (C,F). Meanwhile, ATP release from WT on the particular stimulus was statistically indistinguishable (P>0.05) from that exhibited by Panx$^{-/-}$ taste buds (compare respective bars in C and F). (**G**) Left panel, representative whole-cell (WC) currents indicating that an assayed taste cell is of type II. The cell isolated from a CV papilla of Panx1-null mice was polarized by 100-ms voltage pulses of between −100 and 50 mV. Right panel: concurrent recordings of WC current (middle trace) from the same taste cell (G) and Fluo-4 fluorescence in a nearby COS-1 cell (bottom trace). Upper trace illustrates the time course of holding potential. The recording conditions were as in Fig. 5B. (**H**) Averaged responses of the ATP-biosensor on depolarization of nearby taste cells via the patch pipette or by 100 mM KCl. The first two bars summarize experiments with individual WT taste cells, and the last two represent experiments with Panx$^{-/-}$ taste cells. The particular stimulation – electrical or by KCl – of individual Panx$^{-/-}$ taste cells elicited ATP-sensor responses that were statistically indistinguishable (P>0.05) from those obtained in experiments with WT taste cells. In all cases, cells were isolated from CV papillae.

the mechanical disturbance of taste buds due to chamber perfusion with control bath solution never evoked detectable ATP secretion (not shown). This pointed out that ATP was specifically released by depolarized taste cells of the type II. The consequent taste stimulation with the taste mixture (100 μm cycloheximide +100 μm neotam +300 μm SC45647) triggered detectable ATP release in 10 out of 26 taste buds (38%) (Fig. 6B, right panel). As summarized in Fig. 6C, ATP release from WT taste buds was dependent on KCl concentration, i.e. on membrane voltage, and the taste mixture was less effective in stimulating ATP liberation. In addition, 9 fungiform taste buds were assayed, and 3 of them released ATP in response to the mix of artificial sweeteners: 100 μM neotam +300 μM SC45647 (not shown). Thus, our approach appeared to be appropriate for stimulating and monitoring ATP secretion from individual taste buds.

Similar experiments were carried out with taste buds (n=12) isolated from CV papillae of Panx1$^{-/-}$ mice (Fig. 6D, left panel). In light of the current concept on the role of Panx1 in taste, it was surprising that taste buds devoid of Panx1 were still capable of liberating ATP on depolarization and on taste stimulation (Fig. 6E). Moreover, Panx1$^{-/-}$ and WT taste buds exhibited comparable, in terms of ATP-sensor responses, ATP release on 70 or 100 mM KCl or the taste mixture (Fig. 6C,F). Particularly, all assayed Panx1$^{-/-}$ taste buds released ATP on depolarization with KCl, and 5 of them (42%) liberated the neurotransmitter in response to taste stimulation.

We also studied ATP release in individual taste cells isolated from CV papillae of Panx1-null mice. It should be noted that WT taste cells can be identified electrophysiologically based on a family of VG currents they exhibited (Romanov and Kolesnikov, 2006; Romanov et al., 2007; Romanov et al., 2008). In particular, when dialyzed with a solution containing 140 mM CsCl, only taste cells of the type II were capable of generating large outward currents. Therefore, we first analyzed whether genetic ablation of Panx1 entailed any change in the electrophysiological profile of type II cells. We found finally no statistically significant difference between type II cells from CV papillae of WT and Panx1-KO mice in their electrophysiology. Specifically, VG currents in cells deficient in Panx1 were on average of the same level and kinetics (Fig. 6G, left panel) compared to WT cells (figure 1 in Romanov et al., 2007).

The voltage-dependent ATP release in individual taste cells devoid of Panx1 was examined using the similar approach. We put taste and COS-1 cells into the same chamber and undertook a preliminary search for type II cells based on their morphology. Next, a given cell of the type II, should the initial identification be confirmed by a perforated patch-clamp recording (Fig. 6G, left panel), was placed in close vicinity of an ATP-responsive COS-1 cell to monitor ATP secretion. Note that only cells with robust VG outward currents were assayed for ATP release. Of 16 cells of the type II tested, 14 (87%) cells released ATP on their depolarization via the patch pipette (Fig. 6F, right panel). In many cases, normal taste cells or taste cells devoid of Panx1 were stimulated by 100 mM KCl, and some cells exhibiting ATP release upon stimulation were identified electrophysiologically (n=4 in each case). Expectedly, all these ATP-secreting taste cells were found to be of the type II by their WC currents.

From the statistical point of view, the genetic ablation of Panx1 expression insignificantly affected the ability of type II cells to release ATP. Indeed, in previous studies of ATP secretion in WT cells of the type II, we found that most (84%) of robust

cells released ATP on depolarization (Romanov et al., 2007). In the present study, 87% of type II cells from Panx1$^{-/-}$ mice exhibited robust ATP release. Moreover, taste cells from WT and Panx1$^{-/-}$ mice were virtually indistinguishable by the intensity of ATP release (Fig. 6H), in terms of averaged responses of the ATP-biosensor (Fig. 6H). Thus, assaying both individual taste cells (Fig. 6G) and taste buds (Fig. 6D–F) provided no evidence in support of Panx1 as a primary subunit of ATP-permeable channels mediating ATP release in taste cells.

Discussion

Mammalian taste cells are markedly distinct from other axonless sensory cells by afferent output. Retinal rods and cones and auditory hair cells employ classical chemical synapses with the principal neurotransmitter glutamate liberating via the Ca^{2+}-dependent exocytotic mechanism. Yet, they do not generate action potentials (APs) upon sensory stimulation but produce graded generator potentials to control tonic release of glutamate (Sterling and Matthews, 2005). In the taste bud, principal chemosensory cells of the type II, which specialize in recognition of bitter, sweet, and umami substances, do generate APs (Vandenbeuch and Kinnamon, 2009) but do not form the conventional synapses with afferent nerve endings. Instead, these taste cells release the afferent neurotransmitter ATP through voltage-gated ATP-permeable channels (Huang et al., 2007; Romanov et al., 2007).

The ATP secretory machinery in taste cells is strongly voltage-dependent and operates highly effectively at low intracellular Ca^{2+} (Romanov et al., 2007; Romanov et al., 2008). Meanwhile, Ca^{2+} mobilization, a key intermediated event in taste transduction, precedes taste cell depolarization and ATP release (Huang et al., 2007). What might be a role of taste-related Ca^{2+} signaling in ATP secretion? In type II cells devoid of the transduction channel TRPM5, taste stimulation elicited robust Ca^{2+} transients but failed to trigger ATP secretion (Huang and Roper, 2010). Nevertheless, these genetically modified cells were still capable of releasing ATP on high KCl (Huang and Roper, 2010), the depolarizing stimulation affecting intracellular Ca^{2+} subtly (Huang and Roper, 2010; Bystrova et al., 2010). Tastants triggered undetectable ATP secretion in taste cells from P2X2/P2X3 double KO mice, while their depolarization with KCl produced virtually normal ATP release (Huang et al., 2011). Therefore, a Ca^{2+} signal alone is unable to liberate ATP without proper depolarization of a taste cell. It thus appears that the principal role of taste transduction-related Ca^{2+} mobilization is opening TRPM5 in order to depolarize taste cells and stimulate voltage-gated ATP-permeable channels, thereby initiating ATP release. Nevertheless, one cannot rule out the possibility that efficacy of afferent output in type II cell may be modulated in a Ca^{2+}-dependent manner.

Characteristic of ATP secretion is a steep dependence on membrane voltage with the threshold of about −10 mV (Romanov et al., 2007; Romanov et al., 2008). With such voltage dependence, gradual generatory potential alone would be inappropriate for governing afferent output. Indeed, being mediated by transduction channels TRPM5, tastant-evoked depolarization should range between the resting potential of nearly −45 mV and the maximum not exceeding the reversal potential of a TRPM5-mediated current that is close to 0 mV under physiological conditions (Romanov et al., 2007). The significant gap between the resting potential and the ATP release threshold indicates that only saturating taste stimulation would evoke high enough depolarization to liberate ATP effectively. In contrast, moderate depolarization above the threshold of about −40 mV could elicit an AP train. Each AP would briefly depolarize a taste cell to nearly 50 mV, liberating a more or less universal ATP quantum. Thus, AP seems to be an obligatory intracellular event of taste transduction. This point of view is strongly supported by the data of Murata et al. (Murata et al., 2010), which assayed ATP release from an individual taste cell embedded in a fungiform bud that was still attached to a piece of the lingual epithelium. When applied to a taste pore, tastants stimulated ATP release that was markedly inhibited by TTX, a specific blocker of VG Na^+ channels (Murata et al., 2010). In experiments with isolated CV taste cells, TTX affected ATP secretion insignificantly (Huang and Roper, 2010). Perhaps, saturated taste stimuli applied to the whole membrane of a taste cell elicited high enough depolarization to trigger sufficient ATP release.

ATP-permeable channels mediating ATP secretion in type II cells should be properly adjusted to this all-or-nothing strategy, as is the case with VG Ca^{2+} channels in classical discontinuous synapses. Following the initial depolarizing phase of AP, VG Ca^{2+} channels, primarily of P/Q- and N-type, open rapidly (for ~0.1 ms) but transport a small Ca^{2+} current since an electrochemical driving force of Ca^{2+} influx is low at high positive membrane voltage (Reid et al., 2003). Although the electrochemical gradient driving Ca^{2+} ions rises significantly during the repolarizing phase of AP, VG Ca^{2+} channels deactivate. Thus, largely tail currents through VG Ca^{2+} channels with appropriately slow kinetics of deactivation can provide the bulk of Ca^{2+} influx to trigger exocytosis. Given that electrochemical forces for Ca^{2+} influx and ATP efflux vary with membrane voltage similarly, ATP-permeable channels with slow enough deactivation and negligible activity at resting potentials seem to be eminently suitable as a conduit for discontinuous ATP release. This concept is corroborated both by modeling voltage-dependent ATP efflux and by the experimental dependence of ATP secretion from type II cells on membrane voltage (Romanov et al., 2008).

Although it is widely accepted that ATP-permeable channels in type II cells are formed by Panx1, no direct evidence has been obtained so far in support of this idea but solely inhibitory effects of CBX on ATP release (Huang et al., 2007; Dando and Roper, 2009; Murata et al., 2010). The existing biophysical and pharmacological data on Panx1 channels were basically obtained in studies of recombinant Panx1 that was expressed mainly in *Xenopus* oocytes and HEK-293 cells (e.g. Bruzzone et al., 2005; Ma et al., 2009; Qiu and Dahl, 2009) but also in neuroblastoma Neuro2A cells (Iglesias et al., 2009). As reported in these studies, Panx1 channels activate and deactivate rapidly, i.e. within a few milliseconds, and exhibit quite detectable activity at high negative voltages. Such kinetic properties and voltage dependence of Panx1 channels are poorly consistent with our inference that ATP-permeable channels in type II cells should be slowly deactivating and negligibly active at rest. This discrepancy could be resolved if properties of Panx1 channels vary depending on cell-specific microenvironment.

Indeed, in Jurkat cells, Panx1 channels are generally inactive, and their activity is induced only during apoptosis by the caspase cleavage of a specific site within Panx1 (Chekeni et al., 2010). Several different Panx1-binding molecules have been identified, raising a range of interesting possibilities to regulate Panx1 activity. In particular, the direct interaction of actin with the Panx1 C-terminal domain was demonstrated (Bhalla-Gehi et al.,

2010). Panx1 can interact with the other members of the pannexin family, Panx2 and Panx3, in a glycosylation-dependent manner (Penuela et al., 2009). Ample evidence suggests that Panx1 interacts with α1D-adrenergic receptors (Billaud, et al., 2011) and with several components of the multiprotein inflammasome complex, including the P2X7 receptor, caspase-1, caspase-11, and some other proteins (Silverman et al., 2008). In N2A cells, the association of P2X7 and Panx1 and activation of this complex require low extracellular Ca^{2+} (Poornima et al., 2012). The K^+ channel subunit Kvβ3 was identified as a potential interacting partner of Panx1 (Bunse et al., 2005). Interestingly, CBX and probenecid were less effective as Panx1 current inhibitors when Kvbeta3 and Panx1 were co-expressed (Bunse et al., 2009).

To test whether Panx1 is a principal mediator of ATP release in taste cells, we sequentially employed two different approaches. First, we examined biophysical properties of pannexons with the specific focus on their ATP permeability by using different expression systems. Second, we analyzed ATP release in taste cells from Panx1-null versus WT mice. Given that Panx2 and Panx3 are not expressed in taste cells (supplementary material Fig. S4), genetic ablation of Panx1 was expected to result in clear abnormality in ATP secretion. We cloned full-length Panx1 from CV papillae and expressed this channel subunit in cells of three different lines, including HEK-293, CHO and neuroblastoma SK-N-SH. Consistently with observations of others, we found Panx1 channels to activate and deactivate rapidly in each expression system (Fig. 1).

Previously, the Panx1 channel has been identified as a cationic channel of a large unitary conductance: 475 pS in oocytes (Bao et al., 2004), 450 pS in insulinoma cells (Iglesias et al., 2009), and 300 pS in cardiac myocytes (Kienitz et al., 2011). On the contrary, our preliminary recordings (Romanov et al., 2011) suggested that expression of Panx1 in HEK 293 cells resulted in the appearance of ~60 pS anion channels, the observation being completely consistent with the results of Ma et al. (Ma et al., 2012). Here, we confirmed those findings and carried out a more accurate analysis of Panx1 channels. In particular, we showed that as a function of membrane voltage, the single Panx1 channel current exhibited outward rectification (Fig. 3) with two marked slopes of nearly 15 pS and 74 pS at negative and positive voltages, respectively (Fig. 4A). The comparison of integral and single-channel currents (Fig. 4B) revealed the dependence of open probability of Panx1 channels on membrane voltage (Fig. 4C). This dependence indicates that Panx1 channels are poorly suitable for discontinuous ATP release as being too active at resting potentials. Panx1 channels were initially reported as Ca^{2+}-gated (Locovei et al., 2006). In further experiments, Ma et al. (Ma et al., 2009) found Panx1 gating to be virtually independent of intracellular Ca^{2+} in the physiologically relevant range of concentrations. In our experiments, a rise in intracellular Ca^{2+} was accompanied by some inhibition of Panx1 currents rather than by their stimulation (supplementary material Fig. S5). It thus appears that intracellular Ca^{2+} is not a significant factor of Panx1 gating.

The ion substitution experiments (Figs 1, 2) provided clear evidence that Panx1 formed essentially anionic channels that were most likely impermeable to anions of the HEPES size (237 Da) and larger. This raised the question whether recombinant Panx1 channels were permeable enough to transport ATP anions (~500 Da). To ultimately clarify this point, we examined ATP release in Panx1 expressing cells by using ATP-responsive COS-1 cells as the ATP-biosensor. Importantly, neither HEK-293 cells (Fig. 5A) nor cells of the CHO and SK-N-SH lines (supplementary material Fig. S3) showed detectable ATP liberation upon stimulation. Meanwhile, taste cells of the type II exhibited massive ATP release under the same recording conditions (Fig. 5B).

Thus, our results indicate that Panx1 channels as such are insufficiently ATP permeable to mediate ATP release, at least in host cells of three different lines. This implies that the presence of Panx1 in a cell does not guarantee it to be ATP secretive. The consistent fact is that Panx1 is expressed not only in Type II cells but also in a subpopulation of taste cells of the type I and type III. Nevertheless, only type II cells release ATP upon stimulation (Huang et al., 2007; Romanov et al., 2007). On the other hand, the previous studies of mice avoid of Panx1 provide clear evidence that this channel protein is involved in ATP release from the airway epithelia, hippocampal slices, and thymocytes (Santiago et al., 2011; Seminario-Vidal et al., 2011; Qu et al., 2011). However, the molecular nature of ATP pathways in these cellular systems remains undetermined. The reconcilable assumption is that Panx1 alone does not form an ATP-permeable channel, which might be a heteromer of Panx1 and other channel subunits.

Finally, we considered the possibility that taste cells possess certain accessory proteins and/or channel subunits that are necessary to convert the pore of a Panx1-based channel into a conduit with high ATP permeability. Alternatively, taste cells might utilize a Panx1-dependent regulatory circuit to control activity of ATP-permeable channels of non-Panx1 nature. To test this idea, we assayed ATP secretion in taste cells from Panx1-null mice. Because solely type II cells could release ATP (Huang et al., 2007; Romanov et al., 2007), we analyzed taste-related ATP secretion using taste buds as much more responsive to taste stimulation, compared to individual taste cells. Taste buds were stimulated by depolarizing KCl or by tastants, while ambient ATP was monitored with the ATP-biosensor. It turned out that taste buds from WT and Panx$^{-/-}$ mice were statistically indistinguishable in terms of ATP-biosensor responses (Fig. 6A–F). The assay of ATP liberation from individual taste cells also provided no evidence that the genetic ablation of Panx1 led to the failure of the ATP secretory machinery (Fig. 6G,H).

As independent control, we analyzed loading of taste cells with carboxyfluorescein, suggesting ATP-permeable channels to be involved. Typically, in a preparation of taste buds or individual taste cells from WT mice, very few cells, most likely damaged, took up the dye under the resting conditions. The depolarization of taste cells with 100 mM KCl led to the marked staining of their cytoplasm with carboxyfluorescein. In agreement with the above-mentioned results (Fig. 6), taste cells devoid of Panx1 exhibited qualitatively similar depolarization-induced pattern of carboxyfluorescein loading (supplementary material Figs S6, S7).

In conclusion, our overall findings argue against Panx1 as a principal subunit of VG channels responsible for ATP secretion in taste cells of the type II. Although theoretically, other upregulated mechanisms could take over the role of ATP release in Panx1 KO mice, we consider this possibility to be unlikely in taste cells. The genetic ablation of the key signaling proteins, including T1R receptors, PLCβ2 and TRPM5, resulted in the complete inhibition of taste responses of type II cells. This points out that the taste transduction cascade is none-redundant. We see no physiological reason in the usage of redundant afferent output, especially AP-driven, to finalize non-redundant taste

transduction. The important issue however remains: if Panx1 is not involved, why CBX inhibits ATP secretion stimulated by tastants in taste cells (Huang et al., 2007; Dando and Roper, 2009; Murata et al., 2010)? Although at the moment we do not have clear answer, an interesting possibility comes from the recent study by Abascal and Zardoya (Abascal and Zardoya, 2012) on leucine-rich repeat-containing 8 (LRRC8) proteins. Reportedly, these proteins are designed as a fusion of pannexin and a LRR domain. Although LRRC8 functions are largely unknown, the proposed membrane topology includes pannexin-like four transmembrane helices, implying the channel function as well. If so, the novel LRRC8 channel, which may be CBX-sensitive and ATP permeable, may be a wanted candidate for mediating ATP secretion in taste cells.

Materials and Methods

Animals

We used adult *Panx1* knockout (KO) mice of either sex, along with the control WT line of close background (C57Bl6). Panx1 KO mouse line has been generated by crossing the Panx1fl/fl (Panx1$^{+/+}$ mice with three LoxP consensus sequences integrated into the Panx1 gene) with CMV-Cre animals. Ubiquitous expression of the CMV promoter ensured germline deletion of exons 3 and 4 and frame-shift mutation in the *Panx1* gene, as described earlier (Dvorianchikova et al., 2012; Gründken et al., 2011). The loss of Panx 1 in the taste tissue of KO mice was confirmed by RT-PCR (supplementary material Fig. S4). For isolation of taste buds or individual cells, mice were euthanized with CO_2 followed by cervical dislocation before tongues were removed. All experimental protocols were carried out following NIH guidelines in line with protocols approved by the Institutional Animal Care and Use Committees (IACUCs) of University of Miami and by the Animal Care Committee of the Institute of Cell Biophysics, Pushchino.

Panx1 cloning

Full-length cDNA encoding murine Panx1 (GeneBank accession number NM 019482.2) was cloned from mouse circumvallate papillae by RT-PCR using primers 5′-TATGCTAGCGCCTTGACCATGG-3′ and 5′-CCAGAATTCAAG-AAGGAAACCATTAGC-3′, and subcloned into the *Nhe*I and *Eco*RI sites of pIRES2-EGFP plasmid vector (Clontech). Total RNA was extracted from mouse circumvallate papillae using the RNeasy mini kit (Qiagen). The isolated RNA was reverse-transcribed with an oligo-dT primer and Superscript RT (Invitrogen) according to the manufacturer's protocol and was used as a template for PCR with Pfx DNA polymerase (Invitrogen). The full-length 1304-bp amplified fragment was validated by sequencing.

Cell culture

The COS-1, HEK-293, CHO and SK-N-SH (Human Brain Neuroblastoma) cell lines were routinely cultured in the Dulbecco's modified Eagle's medium (DMEM; Invitrogen) and F12 medium (Gibco) containing 10% (vol/vol) fetal bovine serum (HyClone), glutamine (1%) and the antibiotic gentamicin (100 μg/ml) (Invitrogen) in 12-well culture plates. Cells were grown in a humidified atmosphere (5% CO_2, 95% O_2) at 37℃.

Transfection

Before the day of transfection, cells were put in 12-well culture plates at the density of 3–5×10^5 cells. The plasmid DNA was transiently transfected into cultured HEK-293 and SK-N-SH cells by replacing the growth medium with the transfection mixture, containing 1.6 μg of DNA +4 μl of Lipofectamine (Invitrogen) in 1 ml of serum-free DMEM. After 4 hours incubation, the transfection mixture was replaced with the normal culture medium. The transfection of CHO cells was carried out with Unifectin-56 (Unifect Group) at 3 μl/1 μg DNA. Cells were assayed 24–72 h after transfection.

Electrophysiology

Transfected cells were identified by EGFP fluorescence and assayed with the patch-clamp technique using the WC or inside-out configuration. Ion currents were recorded, filtered, and analyzed using an Axopatch 200 B amplifier, a DigiData 1322 interface, and the pClamp8 software (Axon Instruments). Intracellular solution contained (mM) 100 CsCl, 1 MgATP, 10 BAPTA-40 CsOH, 10 HEPES–CsOH, pH 7.4. Taste cells were assayed using the perforated patch approach with the recording pipette containing (mM): 140 CsCl, 0.6 $MgCl_2$, 0.5 EGTA, 10 HEPES-CsOH (pH 7.4), 400 μg/ml amphotericin B. Cells were stimulated by bath application of compounds. All chemicals were from Sigma-Aldrich, except SC45647 that was kindly provided by Prof. R. F. Margolskee. Experiments were carried out at 23–25℃.

ATP-biosensor

Cells of the COS-1 line, which endogenously express P2Y receptors coupled to Ca^{2+} mobilization, were used as a cellular sensor for monitoring ambient nanomolar ATP (Romanov et al., 2007). Cells were suspended in Hanks's solution containing 0.25% trypsin and collected in a 1.5 ml tube after terminating the reaction with 2% fetal bovine serum (HyClone). Further, cells were placed into recording chamber and loaded with 4 μM Fluo-4AM+15 μg/ml Pluronic (both from Molecular Probes) for 30 min at 23–25℃. Cell fluorescence was excited with a computer controlled light emitting diode (Luxion) at 480 nm and recorded at 535 nm. Sequential fluorescence images were acquired every 0.5–2 seconds using a fluorescent Axioscope-2 microscope, an EMCCD Andor iXON camera (Andor Technology) and Workbench 6.0 software (INDEC Biosystems).

Funding

This work was supported by the Russian Academy of Sciences (Programs 'Molecular and Cell Biology' and 'Mechanisms of integration of molecular systems mediating physiological functions'); the Russian Foundation for Basic Research [grant numbers 11-04-00057, 10-04-01230, 10-04-01105]; and the National Institutes of Health [grant number EY021517]. Deposited in PMC for release after 12 months.

Supplementary material available online at
http://jcs.biologists.org/lookup/suppl/doi:10.1242/jcs.111062/-/DC1

References

Abascal, F. and Zardoya, R. (2012). LRRC8 proteins share a common ancestor with pannexins, and may form hexameric channels involved in cell-cell communication. *Bioessays* **34**, 551-560.

Bao, L., Locovei, S. and Dahl, G. (2004). Pannexin membrane channels are mechanosensitive conduits for ATP. *FEBS Lett.* **572**, 65-68.

Baryshnikov, S. G., Rogachevskaja, O. A. and Kolesnikov, S. S. (2003). Calcium signaling mediated by P2Y receptors in mouse taste cells. *J. Neurophysiol.* **90**, 3283-3294.

Bhalla-Gehi, R., Penuela, S., Churko, J. M., Shao, Q. and Laird, D. W. (2010). Pannexin1 and pannexin3 delivery, cell surface dynamics, and cytoskeletal interactions. *J. Biol. Chem.* **285**, 9147-9160.

Billaud, M., Lohman, A. W., Straub, A. C., Looft-Wilson, R., Johnstone, S. R., Araj, C. A., Best, A. K., Chekeni, F. B., Ravichandran, K. S., Penuela, S. et al. (2011). Pannexin1 regulates α1-adrenergic receptor- mediated vasoconstriction. *Circ. Res.* **109**, 80-85.

Bo, X., Alavi, A., Xiang, Z., Oglesby, I., Ford, A. and Burnstock, G. (1999). Localization of ATP-gated $P2X_2$ and $P2X_3$ receptor immunoreactive nerves in rat taste buds. *Neuroreport* **10**, 1107-1111.

Bruzzone, R., Barbe, M. T., Jakob, N. J. and Monyer, H. (2005). Pharmacological properties of homomeric and heteromeric pannexin hemichannels expressed in Xenopus oocytes. *J. Neurochem.* **92**, 1033-1043.

Bunse, S., Haghika, A., Zoidl, G. and Dermietzel, R. (2005). Identification of a potential regulator of the gap junction protein pannexin1. *Cell Commun. Adhes.* **12**, 231-236.

Bunse, S., Locovei, S., Schmidt, M., Qiu, F., Zoidl, G., Dahl, G. and Dermietzel, R. (2009). The potassium channel subunit Kvbeta3 interacts with pannexin 1 and attenuates its sensitivity to changes in redox potentials. *FEBS J.* **276**, 6258-6270.

Bystrova, M. F., Yatzenko, Y. E., Fedorov, I. V., Rogachevskaja, O. A. and Kolesnikov, S. S. (2006). P2Y isoforms operative in mouse taste cells. *Cell Tissue Res.* **323**, 377-382.

Chaudhari, N. and Roper, S. D. (2010). The cell biology of taste. *J. Cell Biol.* **190**, 285-296.

Chekeni, F. B., Elliott, M. R., Sandilos, J. K., Walk, S. F., Kinchen, J. M., Lazarowski, E. R., Armstrong, A. J., Penuela, S., Laird, D. W., Salvesen, G. S. et al. (2010). Pannexin 1 channels mediate 'find-me' signal release and membrane permeability during apoptosis. *Nature* **467**, 863-867.

D'hondt, C., Ponsaerts, R., De Smedt, H., Vinken, M., De Vuyst, E., De Bock, M., Wang, N., Rogiers, V., Leybaert, L., Himpens, B. et al. (2011). Pannexin channels in ATP release and beyond: an unexpected rendezvous at the endoplasmic reticulum. *Cell. Signal.* **23**, 305-316.

Dahl, G. and Locovei, S. (2006). Pannexin: to gap or not to gap, is that a question? *IUBMB Life* **58**, 409-419.

Dando, R. and Roper, S. D. (2009). Cell-to-cell communication in intact taste buds through ATP signalling from pannexin 1 gap junction hemichannels. *J. Physiol.* **587**, 5899-5906.

Dvoriantchikova, G., Ivanov, D., Barakat, D., Grinberg, A., Wen, R., Slepak, V. Z. and Shestopalov, V. I. (2012). Genetic ablation of Pannexin1 protects retinal neurons from ischemic injury. *PLoS ONE* **7**, e31991.

Finger, T. E., Danilova, V., Barrows, J., Bartel, D. L., Vigers, A. J., Stone, L., Hellekant, G. and Kinnamon, S. C. (2005). ATP signaling is crucial for communication from taste buds to gustatory nerves. *Science* **310**, 1495-1499.

Gründken, C., Hanske, J., Wengel, S., Reuter, W., Abdulazim, A., Shestopalov, V. I., Dermietzel, R., Zoidl, G. and Prochnow, N. (2011). Unified patch clamp

protocol for the characterization of Pannexin 1 channels in isolated cells and acute brain slices. *J. Neurosci. Methods* **199**, 15-25.

Huang, Y. A. and Roper, S. D. (2010). Intracellular Ca($^{2+}$) and TRPM5-mediated membrane depolarization produce ATP secretion from taste receptor cells. *J. Physiol.* **588**, 2343-2350.

Huang, Y. J., Maruyama, Y., Dvoryanchikov, G., Pereira, E., Chaudhari, N. and Roper, S. D. (2007). The role of pannexin 1 hemichannels in ATP release and cell-cell communication in mouse taste buds. *Proc. Natl. Acad. Sci. USA* **104**, 6436-6441.

Huang, Y. A., Dando, R. and Roper, S. D. (2009). Autocrine and paracrine roles for ATP and serotonin in mouse taste buds. *J. Neurosci.* **29**, 13909-13918.

Huang, Y. A., Stone, L. M., Pereira, E., Yang, R., Kinnamon, J. C., Dvoryanchikov, G., Chaudhari, N., Finger, T. E., Kinnamon, S. C. and Roper, S. D. (2011). Knocking out P2X receptors reduces transmitter secretion in taste buds. *J. Neurosci.* **31**, 13654-13661.

Iglesias, R., Spray, D. C. and Scemes, E. (2009). Mefloquine blockade of Pannexin1 currents: resolution of a conflict. *Cell Commun. Adhes.* **16**, 131-137.

Iwabuchi, S. and Kawahara, K. (2011). Functional significance of the negative-feedback regulation of ATP release via pannexin-1 hemichannels under ischemic stress in astrocytes. *Neurochem. Int.* **58**, 376-384.

Kataoka, S., Toyono, T., Seta, Y., Ogura, T. and Toyoshima, K. (2004). Expression of $P2Y_1$ receptors in rat taste buds. *Histochem. Cell Biol.* **121**, 419-426.

Kataoka, S., Toyono, T., Seta, Y. and Toyoshima, K. (2006). Expression of ATP-gated P2X3 receptors in rat gustatory papillae and taste buds. *Arch. Histol. Cytol.* **69**, 281-288.

Kienitz, M. C., Bender, K., Dermietzel, R., Pott, L. and Zoidl, G. (2011). Pannexin 1 constitutes the large conductance cation channel of cardiac myocytes. *J. Biol. Chem.* **286**, 290-298.

Locovei, S., Bao, L. and Dahl, G. (2006). Pannexin 1 in erythrocytes: function without a gap. *Proc. Natl. Acad. Sci. USA* **103**, 7655-7659.

Ma, W., Hui, H., Pelegrin, P. and Surprenant, A. (2009). Pharmacological characterization of pannexin-1 currents expressed in mammalian cells. *J. Pharmacol. Exp. Ther.* **328**, 409-418.

Ma, W., Compan, V., Zheng, W., Martin, E., North, R. A., Verkhratsky, A. and Surprenant, A. (2012). Pannexin 1 forms an anion-selective channel. *Pflugers Arch.* **463**, 585-592.

MacVicar, B. A. and Thompson, R. J. (2010). Non-junction functions of pannexin-1 channels. *Trends Neurosci.* **33**, 93-102.

Murata, Y., Yasuo, T., Yoshida, R., Obata, K., Yanagawa, Y., Margolskee, R. F. and Ninomiya, Y. (2010). Action potential-enhanced ATP release from taste cells through hemichannels. *J. Neurophysiol.* **104**, 896-901.

Pelegrin, P. and Surprenant, A. (2006). Pannexin-1 mediates large pore formation and interleukin-1beta release by the ATP-gated P2X7 receptor. *EMBO J.* **25**, 5071-5082.

Penuela, S., Bhalla, R., Nag, K. and Laird, D. W. (2009). Glycosylation regulates pannexin intermixing and cellular localization. *Mol. Biol. Cell* **20**, 4313-4323.

Poornima, V., Madhupriya, M., Kootar, S., Sujatha, G., Kumar, A. and Bera, A. K. (2012). P2X7 receptor-pannexin 1 hemichannel association: effect of extracellular calcium on membrane permeabilization. *J. Mol. Neurosci.* **46**, 585-594.

Qiu, F. and Dahl, G. (2009). A permeant regulating its permeation pore: inhibition of pannexin 1 channels by ATP. *Am. J. Physiol. Cell Physiol.* **296**, C250-C255.

Qu, Y., Misaghi, S., Newton, K., Gilmour, L. L., Louie, S., Cupp, J. E., Dubyak, G. R., Hackos, D. and Dixit, V. M. (2011). Pannexin-1 is required for ATP release during apoptosis but not for inflammasome activation. *J. Immunol.* **186**, 6553-6561.

Ransford, G. A., Fregien, N., Qiu, F., Dahl, G., Conner, G. E. and Salathe, M. (2009). Pannexin 1 contributes to ATP release in airway epithelia. *Am. J. Respir. Cell Mol. Biol.* **41**, 525-534.

Reid, C. A., Bekkers, J. M. and Clements, J. D. (2003). Presynaptic Ca^{2+} channels: a functional patchwork. *Trends Neurosci.* **26**, 683-687.

Romanov, R. A. and Kolesnikov, S. S. (2006). Electrophysiologically identified subpopulations of taste bud cells. *Neurosci. Lett.* **395**, 249-254.

Romanov, R. A., Rogachevskaja, O. A., Bystrova, M. F., Jiang, P., Margolskee, R. F. and Kolesnikov, S. S. (2007). Afferent neurotransmission mediated by hemichannels in mammalian taste cells. *EMBO J.* **26**, 657-667.

Romanov, R. A., Rogachevskaja, O. A., Khokhlov, A. A. and Kolesnikov, S. S. (2008). Voltage dependence of ATP secretion in mammalian taste cells. *J. Gen. Physiol.* **132**, 731-744.

Romanov, R. A., Bystrova, M. F., Rogachevskaja, O. A. and Kolesnikov, S. S. (2011). Channel activity of recombinant pannexin 1. *Biologicheskie Membrany (Moscow)* **28**, 374-381.

Royer, S. M. and Kinnamon, J. C. (1991). HVEM serial-section analysis of rabbit foliate taste buds: I. Type III cells and their synapses. *J. Comp. Neurol.* **306**, 49-72.

Santiago, M. F., Veliskova, J., Patel, N. K., Lutz, S. E., Caille, D., Charollais, A., Meda, P. and Scemes, E. (2011). Targeting pannexin1 improves seizure outcome. *PLoS ONE* **6**, e25178.

Seminario-Vidal, L., Okada, S. F., Sesma, J. I., Kreda, S. M., van Heusden, C. A., Zhu, Y., Jones, L. C., O'Neal, W. K., Penuela, S., Laird, D. W. et al. (2011). Rho signaling regulates pannexin 1-mediated ATP release from airway epithelia. *J. Biol. Chem.* **286**, 26277-26286.

Silverman, W., Locovei, S. and Dahl, G. (2008). Probenecid, a gout remedy, inhibits pannexin 1 channels. *Am. J. Physiol. Cell Physiol.* **295**, C761-C767.

Sridharan, M., Adderley, S. P., Bowles, E. A., Egan, T. M., Stephenson, A. H., Ellsworth, M. L. and Sprague, R. S. (2010). Pannexin 1 is the conduit for low oxygen tension-induced ATP release from human erythrocytes. *Am. J. Physiol. Heart Circ. Physiol.* **299**, H1146-H1152.

Sterling, P. and Matthews, G. (2005). Structure and function of ribbon synapses. *Trends Neurosci.* **28**, 20-29.

Tabata, S., Crowley, H. H., Bottger, B., Finger, T. E., Margolskee, R. F. and Kinnamon, J. C. (1995). Immunoelectron microscopic analysis of gustducin in taste cells of the rat. *Chem. Senses* **20**, 788.

Vandenbeuch, A. and Kinnamon, S. C. (2009). Why do taste cells generate action potentials? *J. Biol.* **8**, 42.

Woehrle, T., Yip, L., Elkhal, A., Sumi, Y., Chen, Y., Yao, Y., Insel, P. A. and Junger W. G. (2010). Pannexin-1 hemichannel-mediated ATP release together with P2X1 and P2X4 receptors regulate T-cell activation at the immune synapse. *Blood*, **116**, 3475-3484.